AD-A131 148 ION-ION RECOMBINATION RATE IN THE EMP SOURCE REGION(U) 1/1
MISSION RESEARCH CORP SANTA BARBARA CA
J G CHERVENAK ET AL. 10 FEB 82 MRC/SD-R-98 DNA-TR-81-83
UNCLASSIFIED DNA001-81-C-0175 F/G 20/14 NL

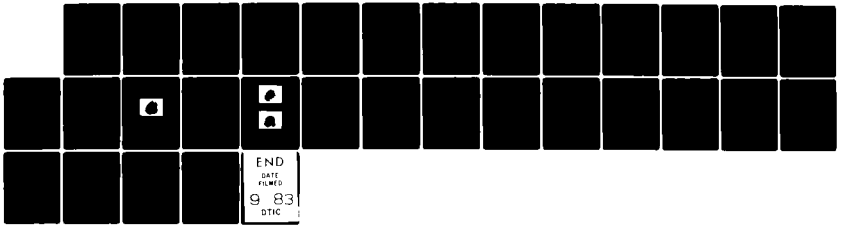

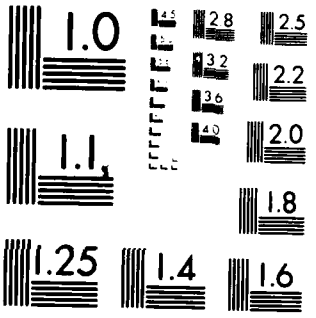

MICROCOPY RESOLUTION TEST CHART
NATIONAL BUREAU OF STANDARDS 1963-A

AD-E 301203

(12)

AD A131148

DNA-TR-81-83

ION-ION RECOMBINATION RATE IN THE EMP SOURCE REGION

J. G. Chervenak
V. A. J. van Lint
Mission Research Corporation
5434 Ruffin Road
San Diego, California 92123

10 February 1982

Technical Report

CONTRACT No. DNA 001-81-C-0175

APPROVED FOR PUBLIC RELEASE;
DISTRIBUTION UNLIMITED.

THIS WORK WAS SPONSORED BY THE DEFENSE NUCLEAR AGENCY
UNDER RDT&E RMSS CODE B326081466 X99QAXVC00002 H2590D.

DTIC FILE COPY

Prepared for
Director
DEFENSE NUCLEAR AGENCY
Washington, DC 20305

DTIC
ELECTE
AUG 8 1983
S D
B

83 07 13 011

UNCLASSIFIED

SECURITY CLASSIFICATION OF THIS PAGE (When Data Entered)

REPORT DOCUMENTATION PAGE		READ INSTRUCTIONS BEFORE COMPLETING FORM
1. REPORT NUMBER DNA-TR-81-83	2. GOVT ACCESSION NO. AD-A131 145	3. RECIPIENT'S CATALOG NUMBER
4. TITLE (and Subtitle) ION-ION RECOMBINATION RATE IN THE EMP SOURCE REGION		5. TYPE OF REPORT & PERIOD COVERED Technical Report 6. PERFORMING ORG. REPORT NUMBER MRC/SD-R-98
7. AUTHOR(s) J.G. Chervenak V.A.J. van Lint		8. CONTRACT OR GRANT NUMBER(s) DNA 001-81-C-0175
9. PERFORMING ORGANIZATION NAME AND ADDRESS Mission Research Corporation 5434 Ruffin Road San Diego, CA 92123		10. PROGRAM ELEMENT, PROJECT, TASK AREA & WORK UNIT NUMBERS Task X99QAXVC-00002
11. CONTROLLING OFFICE NAME AND ADDRESS Director Defense Nuclear Agency Washington, D.C. 20305		12. REPORT DATE 10 February 1982 13. NUMBER OF PAGES 32
14. MONITORING AGENCY NAME & ADDRESS(if different from Controlling Office)		15. SECURITY CLASS (of this report) UNCLASSIFIED 15a. DECLASSIFICATION/DOWNGRADING SCHEDULE N/A since UNCLASSIFIED

16. DISTRIBUTION STATEMENT (of this Report)

Approved for public release distribution unlimited.

17. DISTRIBUTION STATEMENT (of the abstract entered in Block 20, if different from Report)

18. SUPPLEMENTARY NOTES

This work was sponsored by the Defense Nuclear Agency under RDT&E RMSS Code B326081466 X99QAXVC00002 H2590D

19. KEY WORDS (Continue on reverse side if necessary and identify by block number)

Source Region EMP
Ion Conductivity
Ion-ion Recombination
Air

20. ABSTRACT (Continue on reverse side if necessary and identify by block number)

The ion-ion recombination coefficient in air was measured to be $7.0 \pm 0.4 \times 10^{-7}$ cm^3/s using an ion chamber at HIFX. The difference between this and previously measured values may be due to air purity or a dose dependence.

DD FORM 1 JAN 73 1473 EDITION OF 1 NOV 65 IS OBSOLETE

UNCLASSIFIED

SECURITY CLASSIFICATION OF THIS PAGE (When Data Entered)

TABLE OF CONTENTS

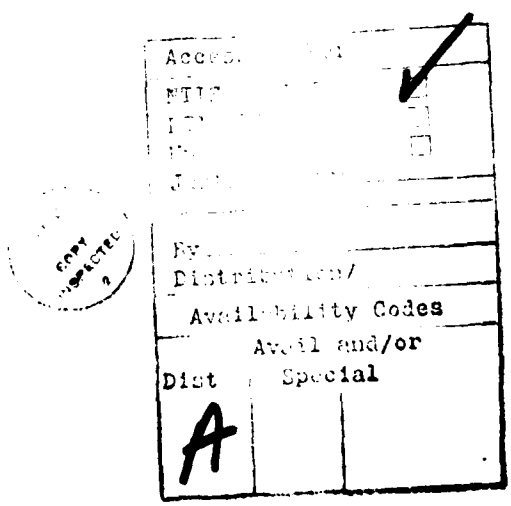

LIST OF ILLUSTRATIONS

SECTION 1
INTRODUCTION

The quasi-static EMP field, and thus all coupled voltages and currents, are inversely proportional to the conductivity of the air in the source region. At late times the air conductivity is dominated by the ion conductivity, which is linear with the ion mobility, μ, and the ion density. For a constant dose rate, $\dot{\gamma}$, the ion density is given by

$$N = \sqrt{\frac{K\dot{\gamma}}{\beta}}$$

where, for air at atmospheric pressure and 20°C, $K = 2.2 \times 10^9$ cm^{-3}/rad and β is the ion-ion recombination coefficient. Thus the ion-ion recombination coefficient is a primary parameter in the theory of late-time EMP.

The value of β in air, presently accepted and used in EMP codes, is that measured by Sayers (Ref. 1). He found that the value of the ion-ion recombination coefficient decreased with increasing initial ionization but reported the low dose (≈1 mrad) value as that for normal air. In this work we are reporting on a measurement of β in air recently made at the HIFX flash x-ray facility. We find a value for β that is 3.2 times lower than that of Sayers.

SECTION 2
HIFX EXPERIMENT

A double-sided, "pie-pan", ionization chamber was used to measure the ion current. This chamber shown in Figure 1 was originally designed for measurement of the electron current during and soon after an ionization pulse. In this experiment the gap between the positive center electrode and the two ground electrodes was 1.4 ± 0.1 cm as measured both before and after the experiment. At room temperature a typical diffusion coefficient for air is ≈0.1 cm^2/s, giving a diffusion length of 0.03 cm at 10 ms, the longest measurement time used in this experiment. Thus the loss of ions by collisional neutralization with the walls and lateral diffusion effects are negligible.

The ionization was produced in the chamber by a collimated beam of bremsstrahlung from the HIFX flash x-ray facility of Harry Diamond Laboratories. The photon spectrum is produced by bremsstrahlung from ≈2 MeV electrons filtered by the target and Al end-plate (Ref. 2). The geometry of the experiment is shown in Figure 2. The purpose of the Al liner in the Pb collimator is to reduce the amount of Compton scattered radiation striking the chamber.

The area of the chamber front plate that is inside the Pb collimator is 275 cm^2. If the area included rays that traversed less than one e-folding of attenuation in the Pb, the area would be 305 cm^2. We take the area at the front plate to be 275 ± 30 cm^2. The initial ion density produced in the chamber depends upon the product of the area at the front plate times the dose measured at the front plate, but the ion current measured

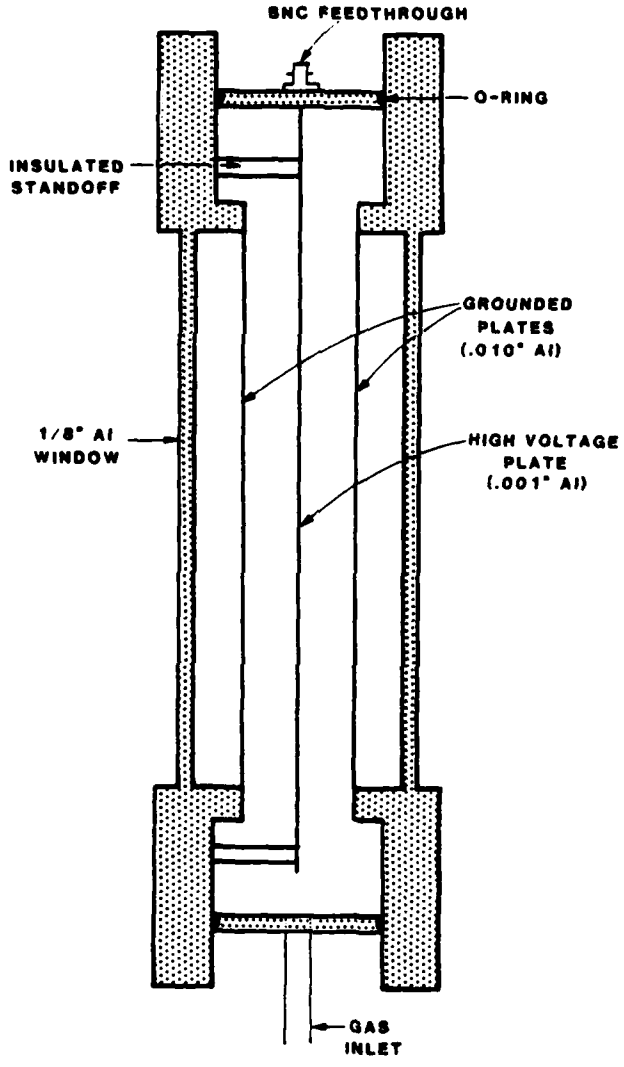

Figure 1. A not-to-scale drawing of the side view of the parallel plate ion chamber.

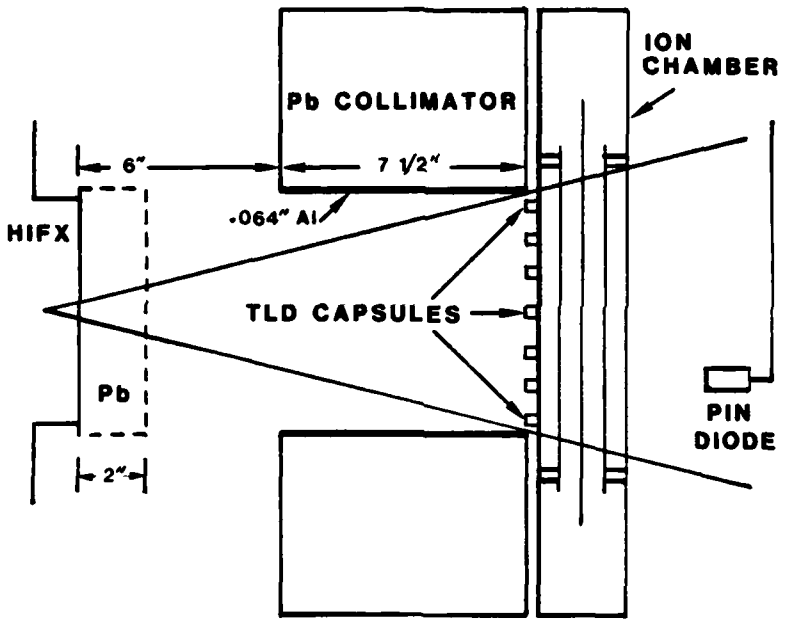

Figure 2. Geometry of experiment.

after significant decay of the ion density depends upon the area of the beam at the center electrode. Assuming that the HIFX beam falls off as $1/r^2$ at the distance of the chamber with an effective point source located 1" behind the HIFX window, the exposure area on the center electrode is 325 cm^2. This value is very insensitive to the exact location of the source, but it is somewhat more uncertain than the area at the front plate. We take the area at the center electrode to be 325 ± 50 cm^2.

The dose at the front plate of the ion chamber was measured with TLD's enclosed in Al capsules having a thickness of 1 gm/cm^2. The window of the ion chamber is almost of equal thickness, so no correction was needed for attenuation in the Al window. In order to produce a lower dose, 2" of Pb was placed in front of the HIFX window. The high dose was measured to be 47 ± 4 rad/shot with seven TLD's exposed on seven shots. The TLD's were placed in a line across the exposure area, so the uncertainty in the dose reflects beam non-uniformity as well as variation in TLD sensitivity. For the low dose, measurement on 18 shots yielded a dose of 0.67 ± 0.08 rad/shot.

A PIN diode was used to detect variation of the dose from shot to shot. On the shots on which the TLD's were exposed the shot-to-shot standard deviation was 6%.

The chamber was pumped to a pressure of ≈100 mTorr before being filled with dry air. Pressure was measured using a capacitance manometer in the Torr range and a thermocouple gauge in the mTorr range. The chamber was at room temperature, measured to be 22°C.

The ion density in the ion chamber as a function of time after the ≈40 ns wide ionization pulse was inferred from the ion current measured at various delay times after the pulse. The HIFX radiation pulse was used to trigger a timing circuit which closed a transistor switch and applied the high voltage to the ion chamber plates as well as supplying timing signals

for the switches in the measuring circuit. A simplified circuit diagram is shown in Figure 3. The delay between the HIFX trigger and the closing of the high voltage switch (SW 1) was recorded on scope 2. This first timing signal was also used to trigger scope 1 which then recorded the amplifier output during the charging of the plates, the opening of switches 2 and 3, and the ion current. The charge for charging the plates of the chamber and to supply the ion current came from the 1 μF capacitor. Detailed circuit diagrams of the timing, switching, and measuring circuits are given in Figures 4 through 6.

The operation of the circuit is shown in Figure 7, where the circuit was activated without firing HIFX. The lower trace shows the delay between the simulated HIFX trigger and the start of the upper trace, which shows the output of the amplifier. The upper trace starts as switch 1 closes and the plates begin charging. The amplifier is clamped to ground at this time but some of the large transient is coupled through. The charging time constant is ≈2 μs depending on the cable capacitance between the switching circuit and chamber. About 60 μs later the amplifier is unclamped from ground and about 40 μs after this the short across the measuring resistor is removed. At 115 μs after the start of the upper trace the amplifier is measuring the ion current. Figure 7 shows an amplifier offset voltage of ≈0.15 V which was subtracted from the voltage measured during the experiment.

The current measuring ability of the circuit was tested by replacing the ion chamber with a 100 MΩ resistor and applying 300 V. The 3.3 μA value deduced from the amplifier output is within 10% of the expected 3 μA current.

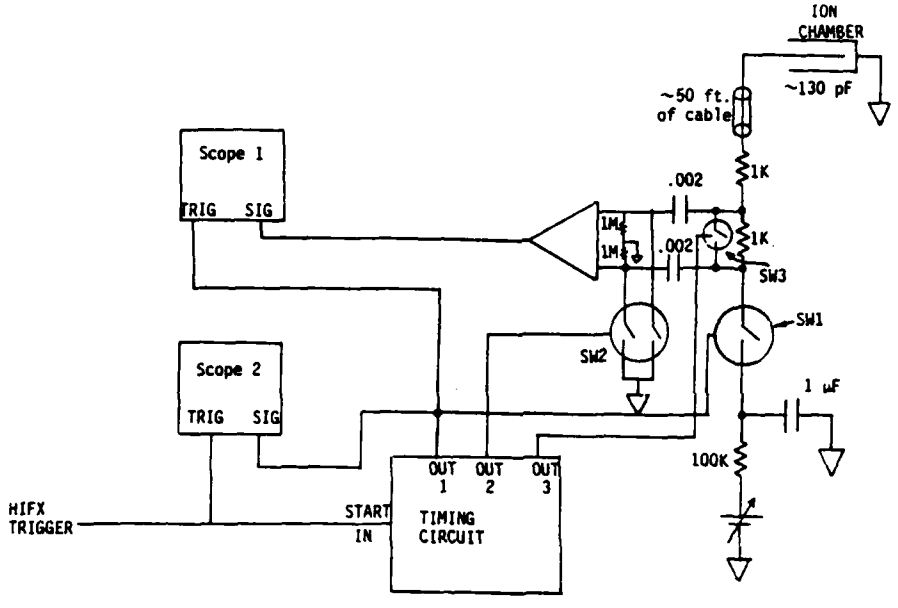

Figure 3. A simplified diagram of the circuit used to measure the ion current at various delay times after the HIFX radiation pulse.

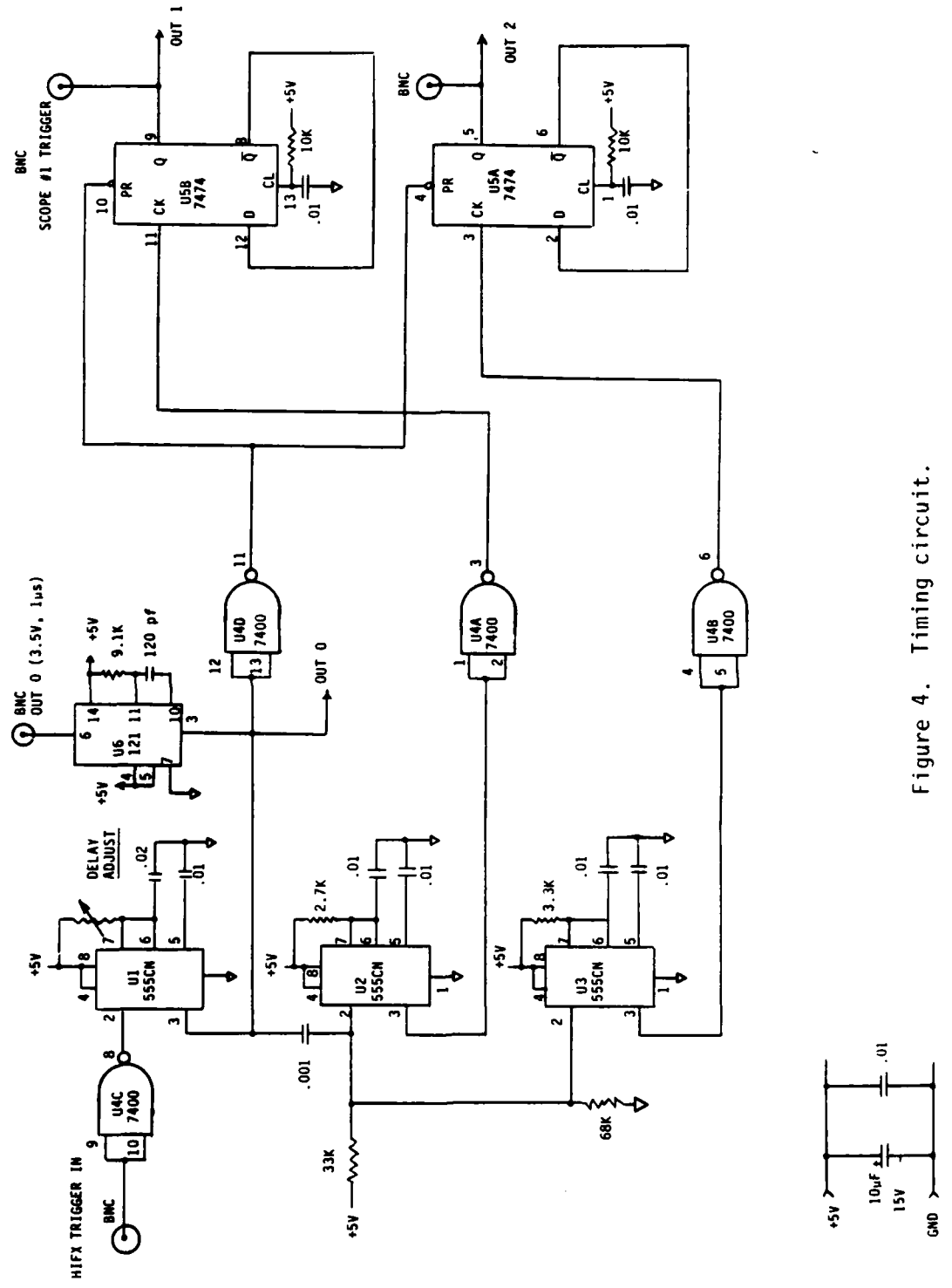

Figure 4. Timing circuit.

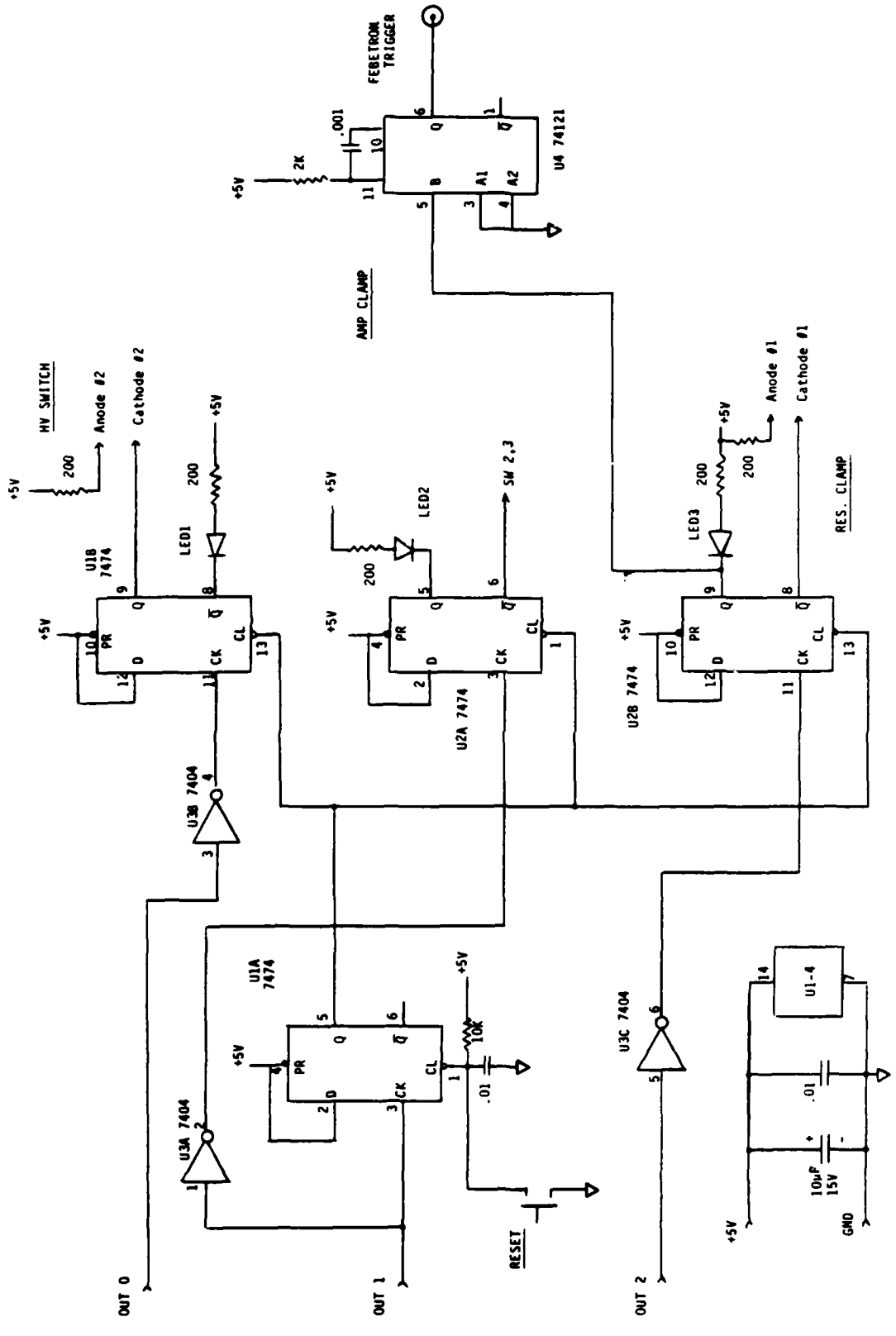

Figure 5. Switch control circuit.

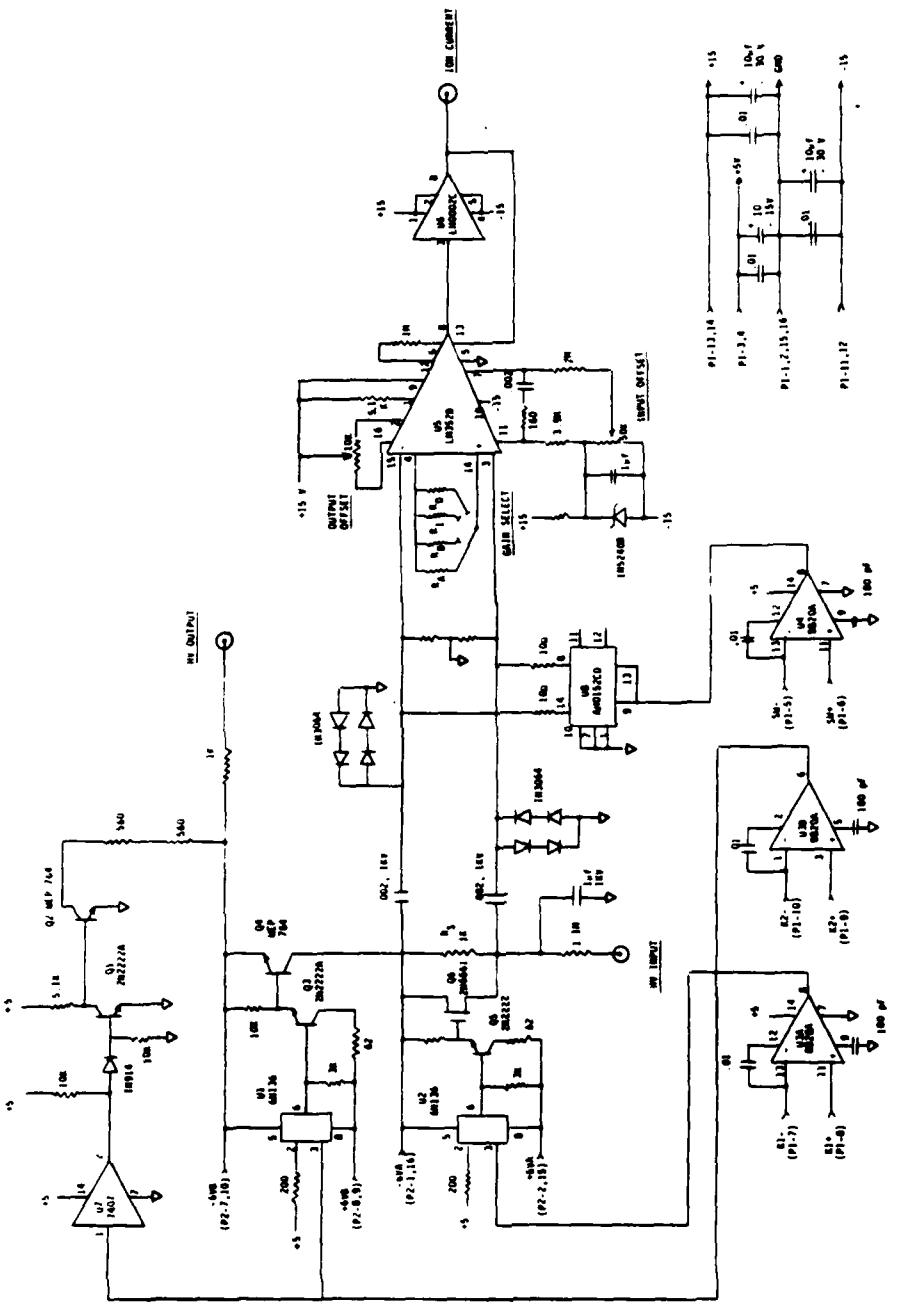

Figure 6. Switching and amplifier circuit.

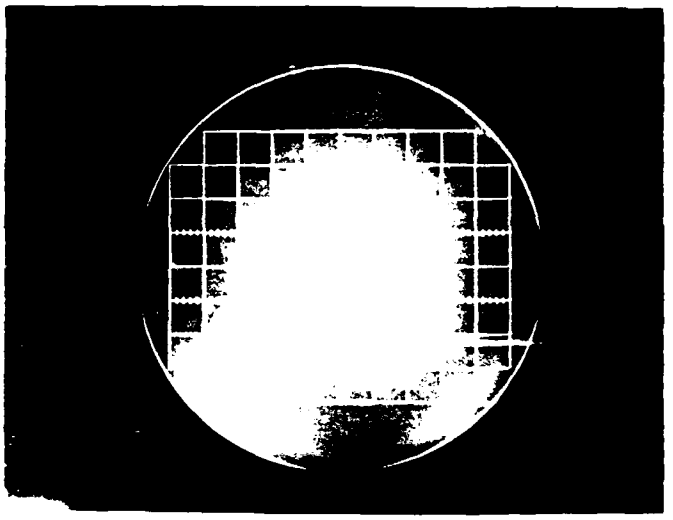

Figure 7. Operation of the measuring circuit in the absence of an ionization pulse. The upper trace (.5 V/div, 50 μs/div) shows the charging of the ion-chamber plates, switching transients, and amplifier offset voltage. The lower trace (5 V/div, 200 μs/div) shows the delay time between the (simulated) HIFX trigger and the charging of the ion chamber plates.

SECTION 3
ION CURRENT AND DENSITY

The decay of the density of ions in the chamber was recorded in two ways in this experiment. At early times, where the ion density decreased significantly during the 400 μs recorded on a single scope sweep, the ion density at a number of times can be obtained from a single HIFX shot. This is demonstrated in Figure 8a where the upper sweep starts at ≈25 μs after HIFX, as shown by the lower trace. A significant reduction in ion current occurs during the time of measurement. In order to measure ion current at later times the delay before application of the voltage was increased. In Figure 8b a delay of 10 ms occurs before the start of the upper trace. In this case the ion density does not change measureably during the sweep time; the ≈2 ms time constant seen in Figure 8b is a circuit relaxation from the input coupling to the amplifier.

After a current at a given time was deduced from the amplifier output voltage, offset voltage, value of measuring resistor (1 KΩ), and amplifier gain setting, up to three more corrections were needed to obtain the true ion current. These are:

1. Sweepout. The current measured in an ion chamber is proportional to the amount of charge moving between the plates. As the ions drift to the electrodes the number of ions are reduced and the current would fall even if the ion density remained constant. The distance that the ions move during a time of application of the field, t_c, is

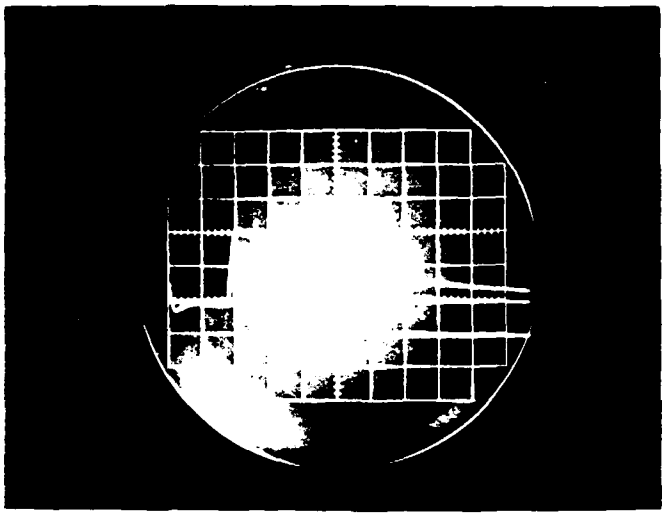

a) Early-time ion current showing decay of ion density. Upper trace: 1 V/div, 50 μs/div. Lower trace: 5 V/div, 20 μs/div. Amplifier gain = 10.

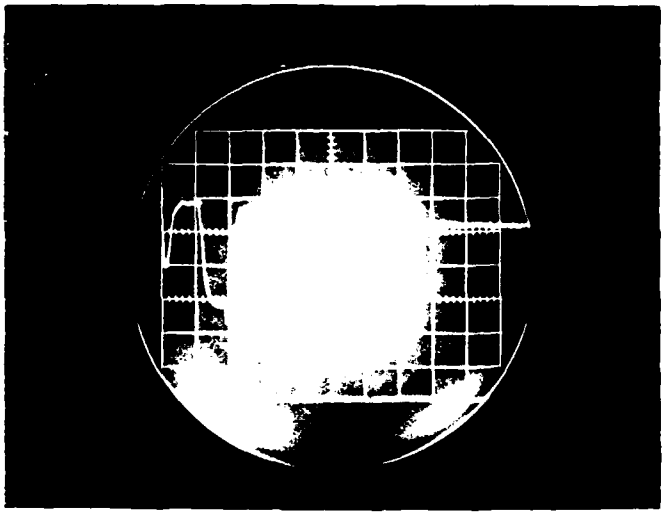

b) Late-time ion current. Decay is due to a circuit time constant. Upper trace: .2 V/div, 50 μs/div. Lower trace: 5 V/div, 2 ms/div. Amplifier gain = 100.

Figure 8. Typical ion-current waveforms.

$$x = \bar{\mu} E t_c \tag{1}$$

where $\bar{\mu}$, the average (over species as well as sign) mobility, is later measured to be 1.7 $cm^2/V \cdot s$. In order to correct for sweepout, measured current was multiplied by d/(d-x), where d is the spacing between the electrodes. The largest sweepout correction was 5%.

2. Boundary layer voltage. During the time that the voltage is applied to the ions before the current measurement is taken, the drift of the ions produce boundary layers at both the cathode and anode. Since the density of ions is decaying according to

$$N(t) = \frac{N(0)}{1 + N(0)\beta t} \tag{2}$$

the average density of ions during a drifting time of t_c, which starts at a delay time t_d after t = 0, is

$$\bar{N} = \frac{1}{t_c \beta} \ln \frac{1 + N(0)\beta(t_d + t_c)}{1 + N(0)\beta t_d} \tag{3}$$

(Note that we are using the notation, $N^+ = N^- = N$) The voltage dropped across the two boundary layers is then given by

$$V_{B.L.} = \frac{e\bar{N}}{2\varepsilon_0} (x_+^2 + x_-^2) \tag{4}$$

where x_+, x_- are the thicknesses of the boundary layers. In order to correct for the reduction in field in the bulk of

the air, measured current was multiplied by $V/(V-V_{B.L.})$. The largest boundary layer correction as 32%.

3. Circuit decay. The circuit had a 2 ms time constant. The measured current was corrected by multiplying by $e^{t/\tau}$ where τ = 2 ms and t was measured from the time at which the shunt was removed from the measuring resistor to the time at which the current was measured. The largest circuit correction was 22%.

The time at which the current was measured ($t_d + t_c$), the measured current, and the corrected ion current are listed in Table 1. The standard conditions of measurement were: 100 V applied voltage, 1 atm pressure, and the high dose from HIFX. Changes to these conditions are indicated in the second column.

In order to determine the ion density from the ion current it is necessary to know the mobility of the ions. On shot 519 the ion current was measured at low dose and early time, such that the initial ion density was reduced only by about 10%. Thus, this constituted a direct (to within the 10% correction) measurement of the ion mobility. The mobility is given by

$$\bar{\mu} = I/4NeEA \qquad (5)$$

Half of the factor of four comes from the two signs of ions and the other half from the double-sided construction of the ion chamber. The 10% correction to N was made by using the value of β that will be found later. N(0) is given by $K\gamma$, where γ is the dose and K is the generation constant. The value found for $\bar{\mu}$ is 1.7 ± 0.3 $cm^2/V \cdot s$. The uncertainty comes mainly from the uncertainty in the area and in the electric field through the uncertainty in the gap width.

Table 1. Measured ion currents, corrections, and ion densities at various delay times.

Shot #	Special Condition	Time (ms)	Measured Current(μA)	Sweep Out Correction	Boundary Layer Correction	Circuit Correction	Ion Current (μA)	N ($10^8 cm^{-3}$)	Uncertainty (±%)
507	low dose	1.12	14.3	1.01	1.00	1.00	14.4	5.6	15
"	low dose	1.50	9.8	1.04	1.04	1.22	12.9	5.0	25
510	low dose	10.1	3.1	1.01	1.00	1.00	3.1	1.2	20
511		10.1	4.1	1.01	1.00	1.00	4.1	1.6	20
512		1.12	35.4	1.01	1.01	1.00	36.2	14	15
"		1.50	20.9	1.04	1.08	1.22	28.6	11	20
513		0.22	136	1.01	1.03	1.00	140	54	15
"		0.35	74.0	1.02	1.11	1.08	90.5	35	20
"		0.60	32.7	1.04	1.32	1.22	54.8	21	30
515		0.14	203	1.01	1.07	1.00	219	84	15
"		0.28	93.1	1.02	1.18	1.08	121	47	20
516		0.14	206	1.01	1.07	1.00	224	86	15
517		3.12	13.2	1.01	1.00	1.00	13.3	5.1	15
518	500V	1.12	162	1.05	1.03	1.00	175	13.5	15
519	low dose	0.14	31.8	1.01	1.00	1.00	32.1	11.8	15
"	low dose	0.28	24.5	1.02	1.02	1.08	27.5	10.1	20
"	low dose	0.52	16.8	1.04	1.07	1.22	22.8	8.3	25
520	0.5 atm	1.12	78.5	1.02	1.02	1.00	83.3	16.1	15
521	0.25 atm	1.12	157	1.04	1.09	1.00	178	17.2	15
522	0.25 atm	10.1	25.7	1.04	1.01	1.00	27.0	2.6	15

Other measurements of mobility of "air ions" agree rather well with this value. Zeleny apparently made the first measurement and found $\mu^+ = 1.4\ cm^2/V \cdot s$ and $\mu^- = 1.9\ cm^2/V \cdot s$ (see Ref. 3). Later measurements made by Bradbury for room air found $\mu^+ = 1.6\ cm^2/V \cdot s$ and $\mu^- = 2.2\ cm^2/V \cdot s$ (see Ref. 4). Although these measurements are suspect as measurements to be compared to theoretical calculations because of problems with impurities, they were made under conditions similar to this experiment.

Having determined the mobility, Equation (5) can now be used to find the ion density from the ion current at any time:

$$N(t) = I(t)/4\pi e EA \qquad (6)$$

The implicit assumption that the mobility is not changing with time will be verified by the results. The second-to-last column in Table 1 gives N as found from Equation (6). For the subatmospheric pressure measurements, the mobility was assumed to scale inversely with pressure.

The uncertainties in N were estimated to be ±15% for the measurements which did not have significant corrections to the currents. Larger uncertainties were assigned to measurements that required large corrections and to the 10 ms measurements which are more uncertain because of the smaller measured voltage compared to the offset voltage.

SECTION 4
RESULTS

The ion density as a function of time from Table 1 are plotted in Figure 9. The solid curves are weighted least square fits of the data to Equation (2). N(0) was calculated from the dose. The high dose data points yield $\beta = 7.0 \pm 0.4 \times 10^{-7}$ cm^3/s and the low dose points yield $\beta = 7.6 \pm 1.1 \times 10^{-7}$ cm^3/s. The uncertainties quoted here are derived from the variation of Chi-squared with β (Ref. 5). For the large intial ionization and the time range of the measurement, the ion density is in the hyperbolic decay region ($N(t) = 1/\beta t$) where the ion density is independent of N(0). In this case the curve of Figure 9 is almost a straight line with a slope of minus one. For the smaller initial ionization, the curve has not yet reached its asymptotic form but is given by Equation (2). Only two points were measured at 0.25 atm; they yield $\beta = 4.4 \pm 0.5 \times 10^{-7}$ cm^3/s.

For comparison the curves that would have resulted from the same values of N(0) but Sayers value of $\beta = 2.3 \times 10^{-6}$ cm^3/s are shown as the dashed lines in Figure 9. We are obviously measuring ion densities that are too large to be consistent with Sayers' value.

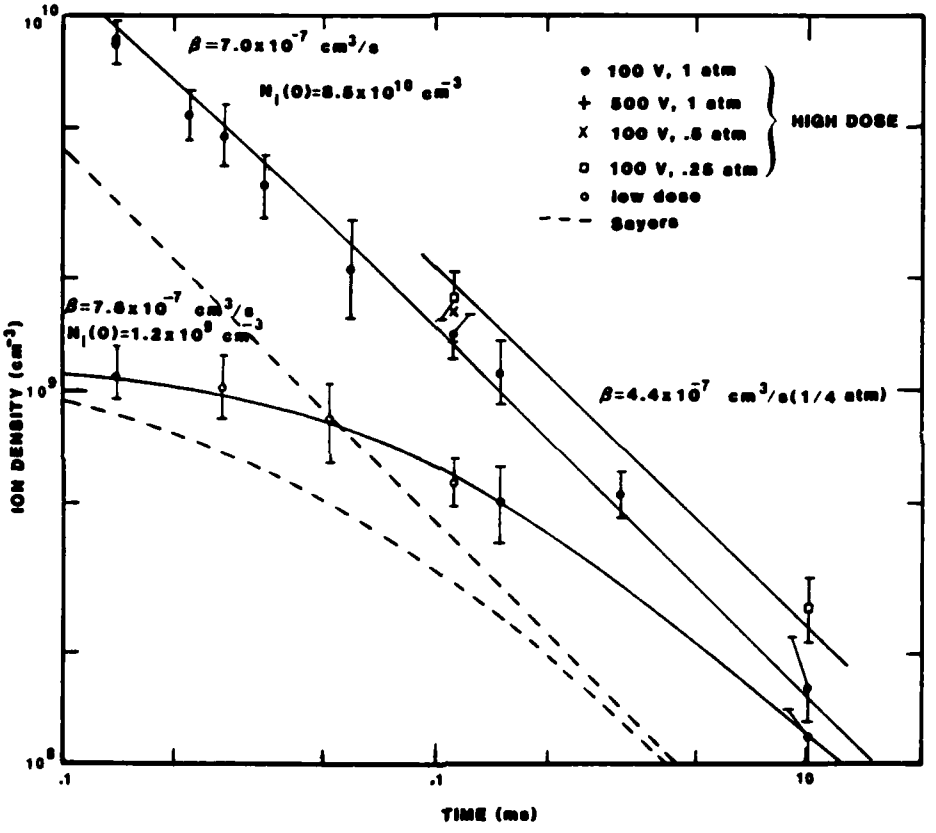

Figure 9. Ion density as a function of time after HIFX ionization pulse.

SECTION 5
DISCUSSION

A fundamental difference between the experiment reported here and that of Sayers is that we measured an ion current and ion mobility to infer the ion density, whereas Sayers collected the ions and measured their charge. There is no obvious reason why these two methods should not give the same results. The good agreement between our value for the ion mobility and previously measured values substantiates the validity of the ion current method. Also the agreement of the data with the functional form of Equation (2) is strong evidence that the mobility is not a function of time over the time range of the experiment.

The magnitude of the ion mobility measured here is also verification that the current measured in the chamber is due only to ions. Because of the much larger mobility of electrons, a small density of free electrons could contribute a current comparable to the ion current, causing too large of a density to be assigned to the ions. However, this electron contamination would also cause the mobility to be anomalously large. The agreement of the data with Equation (2) for the two values of dose rules out an electron concentration which is not a very special function of both the ion density and ion age.

In this experiment measurements were taken at ion densities that did not differ from the initial ion densities by enough orders of magnitude that scattered radiation could increase the collection area of the chamber from that of the collimated area. In particular, the ion density for the low dose curve changes by only one order of magnitude over the time range of the measurement.

In both this and Sayers' experiment, β was measured at room temperature of ≈20°C. Also the ion mobility measured in this experiment was for room temperature; the correction to 0°C (the "reduced mobility") is only 8%.

Another difference between this and Sayers' experiment is the age of the ions. Sayers measured ion densities at times between 10 ms and 500 ms; while the time range in this experiment was from 0.1 ms to 10 ms. Ions are known to cluster with time, however this would be expected to reduce β rather than increase it.

Sayers saw a decrease of β with time out to ≈0.1 s, which he ascribed to columnar and cluster recombination. Assuming that Sayers had x-rays that were approximately three times minimum ionizing (≈50 keV), he had a track density of $\approx 10^4$ tracks/cm^2 or 0.01 cm between tracks. The diffusion time required for the tracks to overlap and produce a uniform ion density is 2 ms. In this experiment we did not see initial recombination because we used x-rays that produced minimum ionizing electrons and a larger dose. Our distance between tracks was $\approx 10^{-4}$ cm for the low dose. This is a smaller distance than the initial distance between a positive ion and its attached electron, $\approx 2 \times 10^{-3}$ cm (Ref. 6). Thus our ion density was initially uniform and no diffusion time is needed to homogenize the ions.

Sayers reports that in his experiment the value of β decreased as the dose was increased and that other investigators saw a decrease in β as the hardness of the x-rays were increased. (Our value of β was also smaller at the higher dose, but not by more than the uncertainty in the measurement.) Sayers attributes this effect to the formation of heavier ions in the air such as ozone and the oxides of nitrogen. Presumably the idea is that impurity molecules are formed in air by radiation and are ionized by charge exchange to form ions that have a much smaller value of β. At a given time, t_m, after the ionization pulse all of the impurity molecules

would be ionized and the ion density would be in the hyperbolic decay region. For a small dose, at t_m there would be a small number of impurity ions and mostly regular ions. For a larger dose, at t_m there would be a larger number of impurity ions and since the total number is independent of the initial number there will be less regular ions. Thus the apparent β would decrease with dose.

In order for this to be a viable explanation, the impurity molecules could not exist in sufficient quantity in the gas prior to irradiation. Sayers used a dose of only ≈1 mrad which will produce 2.2×10^6 ions/cm^3. If an equal number of impurity molecules were formed, they would have a concentration of 1 part per 10^{13} air molecules. Impurities of ozone and oxides of nitrogen much larger than this would be expected to exist in the air used by Sayers. The explanation could still be valid if the impurity is not a naturally occurring molecule or is an excited state of a naturally occurring molecule.

We have previously reported a value for the ion-ion recombination coefficient mesured at HERMES (Ref. 7). This measurement was an adjunct to the measurement of the electron conductivity of highly dosed air and was taken on air that had an intial ion density of $\approx 4 \times 10^{15}$ cm^{-3}. Unfortunately this large difference caused the collection area of the ion chamber to be larger than the collimated area due to scattered radiation.(Ref. 8). The most reasonable assumption in this experiment is that when the initial ion density had decayed from 4×10^{15} to 10^9 cm^{-3} the ions were uniform throughout the space between the electrodes whether or not it was in the beam. Using this assumption and the value of the mobility in the HIFX experiment, we find a value of $\beta = 1.0 \times 10^{-6}$ cm^3/s at 50°C. Correcting this to room temperature (with $\beta \approx T^{-3/2}$) we have $\beta = 1.2 \times 10^{-6}$ cm^3/s. This value has to be viewed as having a much larger uncertainty than the HIFX measurement both because of the uncertainty of the area and the assumption that the mobility is the same as that measured at a much lower dose.

Although Sayers' measurements were performed in 1938, he used a Hg diffusion pump and good vacuum techniques for that time. In the experiment reported here the chamber was not baked out and was only pumped to ≈100 mTorr before being filled with air. McGowen (Ref. 9) has found agreement with Sayers' value of β for air passed over a series of cold traps but a value only half as large for untrapped air. A large part of the difference between our value of β and that of Sayers may well be due to the purity of the air under study. Even though our chamer was filled from a gas bottle of dry, pure air, the gas in the chamber consisted of air with impurities from outgassing of the surfaces, including a small amount of water vapor.

One way to explain our lower value of β is if the impurity ions have a larger mass than the normal air ions. However if this were the case then the mobility of the ions would also be smaller than for pure air. Our measured value of mobility when compared to values measured in pure N_2 and O_2 does not indicate unusually large ions.

SECTION 6
CONCLUSION

There is a significant discrepancy between the value of the ion-ion recombination coefficient measured by Sayers and the one reported here. This results in almost a factor of two difference in the predicted EMP field at late times. The discrepancy may be due to the existence of different ions in the two experiments either because of differences in dose or gas purity.

If there is truly a dose dependence to β, this is of great importance to EMP since the expected dose is up to 10^9 times greater than that used in Sayers' experiment. If the difference is due to air purity then Sayers' high purity value may not be correct for the atmospheric air of interest to EMP. If the relevant impurity is a naturally occurring impurity, then the value of β for "dirty" air is relevant to EMP. If, however, the relevant impurity was artifically introduce by the experiment, e.g., pump oil, then β for air without this impurity is the proper value to be used in EMP calculations.

REFERENCES

1. J. Sayers, Proc. Roy. Soc., A169, 83 (1938).

2. J.V. Rosenfeld, "Tree Simulation Facilities," Defense Nuclear Agency, DNA2432H (January 1979).

3. L.G. Huxley and R.W. Crompton, The Diffusion and Drift of Electrons in Gases, John Wiley and Sons, p.3 (1974). Also in A. von Engle, Ionized Gases, Oxford University Press, p.114 (1965).

4. L.B. Loeb, Basic Processes of Gaseous Electronics, U. of California Press, p.116 (1961).

5. P.R. Bevington, Data Reduction and Error Analysis for the Physical Sciences, McGraw-Hill, p.245 (1969).

6. V.A.J. van Lint, et al., Mechanisms of Radiation Effects in Electronic Materials, John Wiley & Sons, p.178 (1979).

7. J.G. Chervenak and V.A.J. van Lint, "Late-Time Air Chemistry Experiment, Final Report," Mission Research Corporation, MRC/SD-R-64 (October 1980).

8. F. Gilmore, private communication.

9. S. McGowan, Can. J. Phys., 45, 439 (1967).

DISTRIBUTION LIST

DEPARTMENT OF DEFENSE

Defense Nuclear Agency
ATTN: RAEE
ATTN: STNA
ATTN: RAEV
ATTN: NATA
4 cy ATTN: TITL

Defense Tech Info Ctr
12 cy ATTN: DD

DEPARTMENT OF THE ARMY

BMD Systems Command
ATTN: BMDSC-HW
ATTN: BMDSC-AOLIB
ATTN: BMDSC-HLE, R. Webb

Harry Diamond Labs
ATTN: DELHD-NW-E, 21000
ATTN: DELHD-TF
ATTN: DELHD-TA-L, 81100
ATTN: DELHD-NW-EC, 21300
ATTN: DELHD-NW-EB, 21200
ATTN: DELHD-NW-EA, 21100
ATTN: DELHD-NW-EE, 21500
ATTN: 00100, Commander/Tech Dir/Div Dir
ATTN: DELHD-NW-ED, 21400
ATTN: DELHD-NW, J. Bombardt, 20000
ATTN: DELHD-R, 22000
ATTN: NMPO
ATTN: DELHD-NW-P, 20240
ATTN: DELHD-TD, 00102
ATTN: Chief Div 10000
2 cy ATTN: DELHD-NW-RC, 22300

DEPARTMENT OF THE AIR FORCE

Air Force Weapons Lab
ATTN: CA
ATTN: NXS
ATTN: SUL
ATTN: NTYEE, C. Baum
ATTN: NTYEP, W. Page
ATTN: NT
ATTN: NTYE, J. Castillo
ATTN: NTN
ATTN: NTYC, M. Schneider

DEPARTMENT OF ENERGY CONTRACTORS

University of California
Lawrence Livermore National Lab
ATTN: L-153, D. Meeker
ATTN: Tech Info Dept, Library
ATTN: L-96, T. Donich
ATTN: L-156, H. Cabayan
ATTN: L-10, H. Kruger
ATTN: L-156, E. Miller

Sandia National Lab
ATTN: Org 9336, E. Hartman
ATTN: R. Parker
ATTN: C. Vittitoe

DEPARTMENT OF ENERGY CONTRACTORS (Continued)

Los Alamos National Lab
ATTN: MS670, J. Malik
ATTN: B. Noel
ATTN: MS 670, J. Hopkins
ATTN: C. Benton

DEPARTMENT OF DEFENSE CONTRACTORS

Dikewood
ATTN: Tech Library for L. Davis
ATTN: Tech Library
ATTN: Tech Library for C. Jones

Electro-Magnetic Applications, Inc
ATTN: D. Merewether

JAYCOR
ATTN: W. Radaski
ATTN: D. Higgins
ATTN: W. Hobbs

JAYCOR
ATTN: E. Wenaas
ATTN: R. Stahl

Kaman Tempo
ATTN: DASIAC

Mission Research Corp
ATTN: EMP Group
ATTN: W. Crevier
ATTN: C. Longmire
5 cy ATTN: Doc Con

Mission Research Corp
ATTN: B. Passenheim
4 cy ATTN: J. Chervanek
4 cy ATTN: V. van Lint

Pacific-Sierra Research Corp
ATTN: H. Brode, Chairman SAGE
ATTN: L. Schlessinger

R & D Associates
ATTN: M. Grover
ATTN: W. Graham
ATTN: C. Mo
ATTN: W. Karzas
ATTN: Doc Con

Science Applications, Inc
ATTN: E. Parkinson

Science Applications, Inc
ATTN: W. Chadsey

PRECEDING PAGE BLANK-NOT FILMED

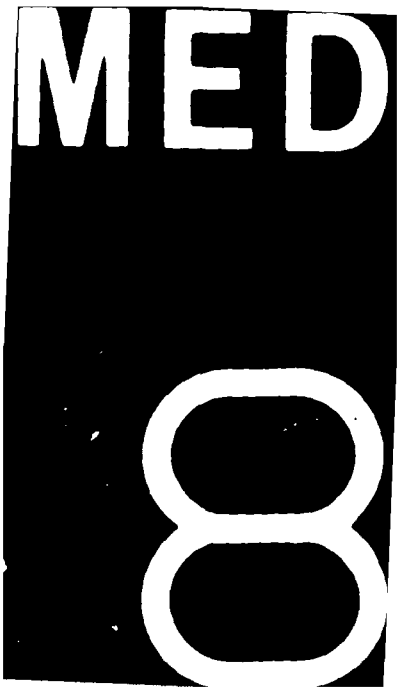
MED
8